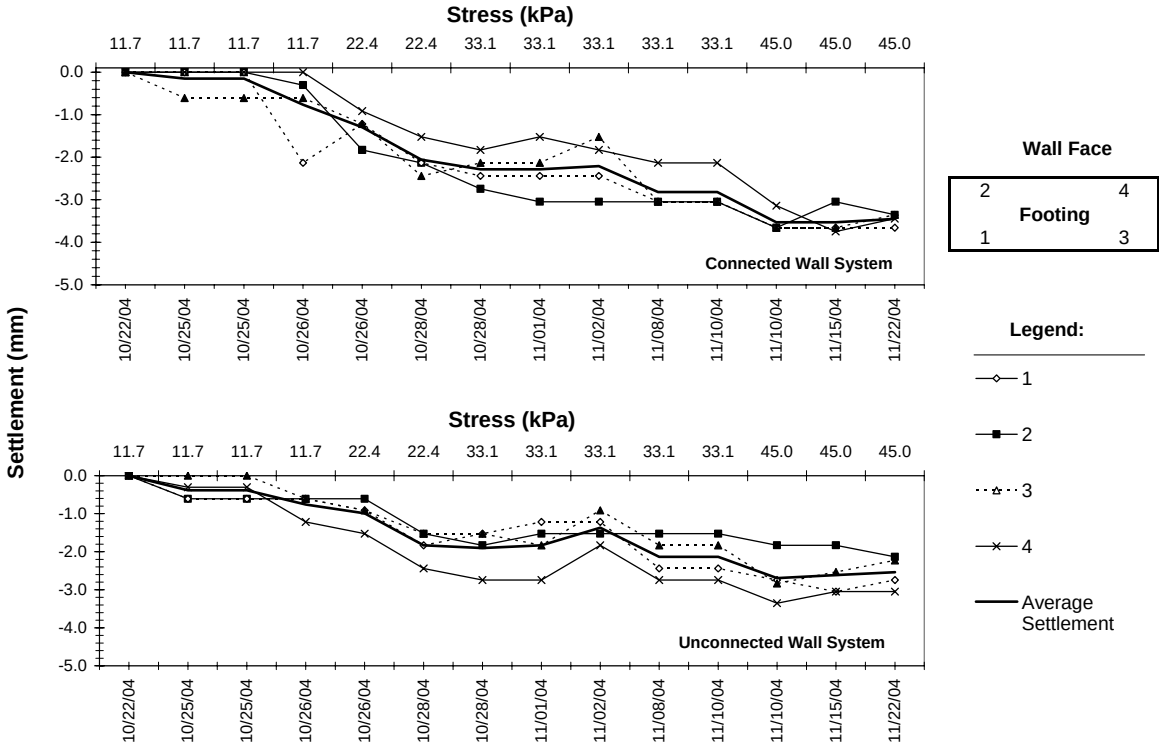


**Figure 59. Graph. Footing settlement measurements recorded during dead loading.**

**Figure 60. Photo. Field-scale test wall load frame and jack set-up.**

## C.6 RESULTS

### C.6.1 Visual Observations

During load testing, it was observed that the geogrid wrap placed at the face of the wall developed slack, as illustrated in figure 61. At various surcharge loadings, the location of the apparent slack appeared to change. No other changes in the MSE wall were visible during load testing.

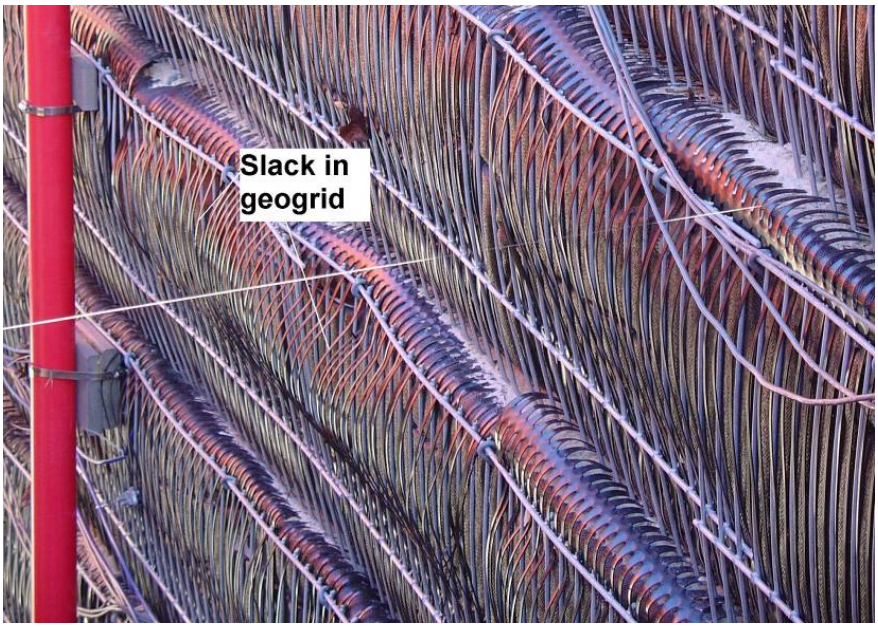


**Figure 61. Photo. Development of slack in geogrid reinforcement during wall loading.**

### C.6.2 Strain Gages

Bonded resistance strain gages were installed on four layers of geogrid near the top, middle and bottom of the wall section, corresponding to lifts 2, 5, 8, and 11 (from bottom to top), and near the front, middle and back of each reinforcing element (i.e., 0.20 m, 0.57 m, and 0.95 m from the face of the MSE wall). Two instrumented sections were selected: one near the center of the connected wall system, and one near the center of the unconnected wall system.

Micro-Measurements EP-series strain gages were installed on the geogrid at the selected locations. The gage selected was a self-temperature-compensated uniaxial strain gage with a length of 500 mils (500GB) having 120 ohm resistivity.

The purpose of the bonded resistance strain gages is to enable evaluation of local stress and strain distribution in the geogrid reinforcing elements and identify areas of maximum stress. Figures 62 and 63 illustrate the strain measurements in the geogrid reinforcements for the connected and unconnected wall systems, respectively.

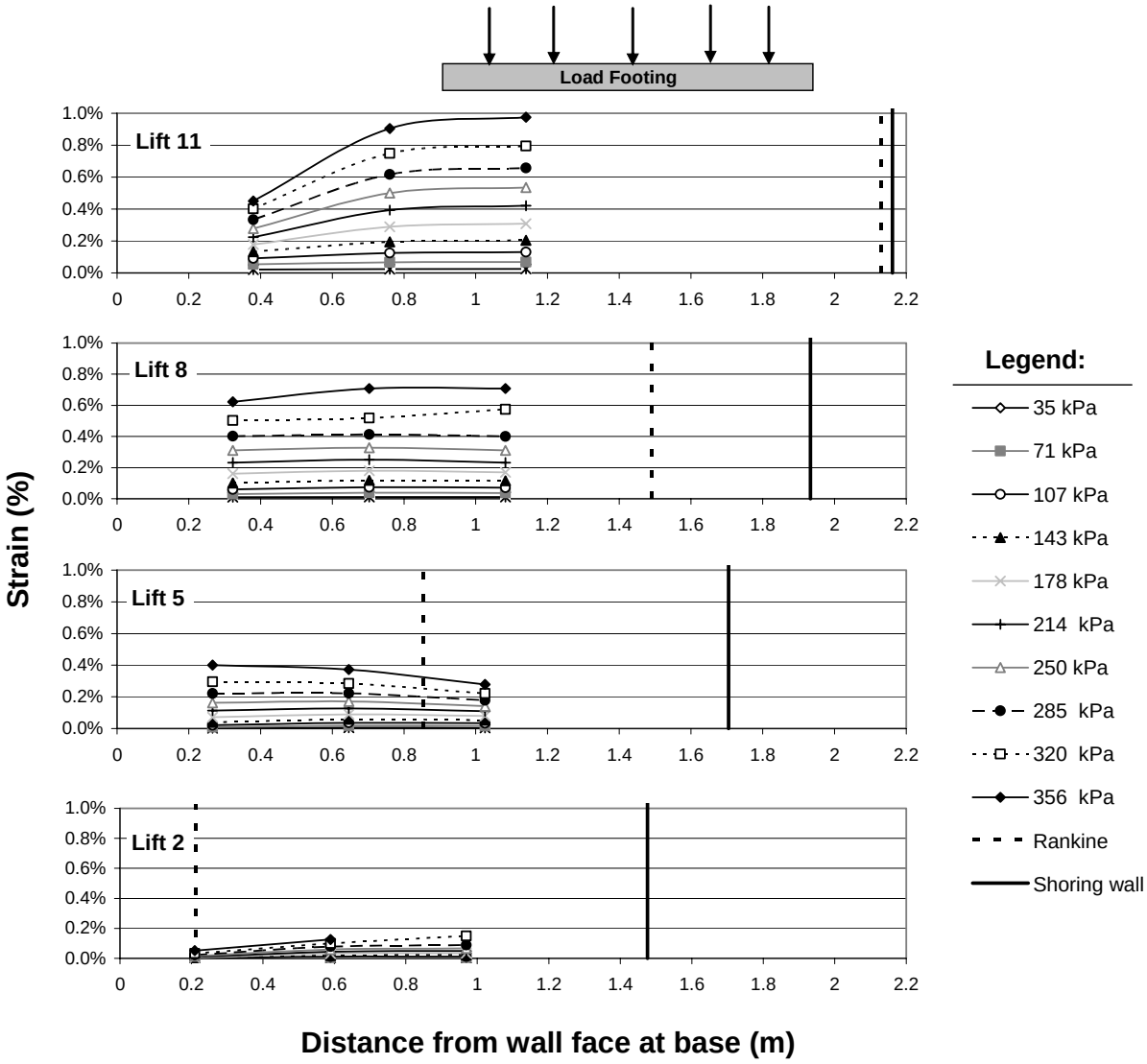


**Figure 62. Graph. Strain measurements in geogrid, connected wall system.**

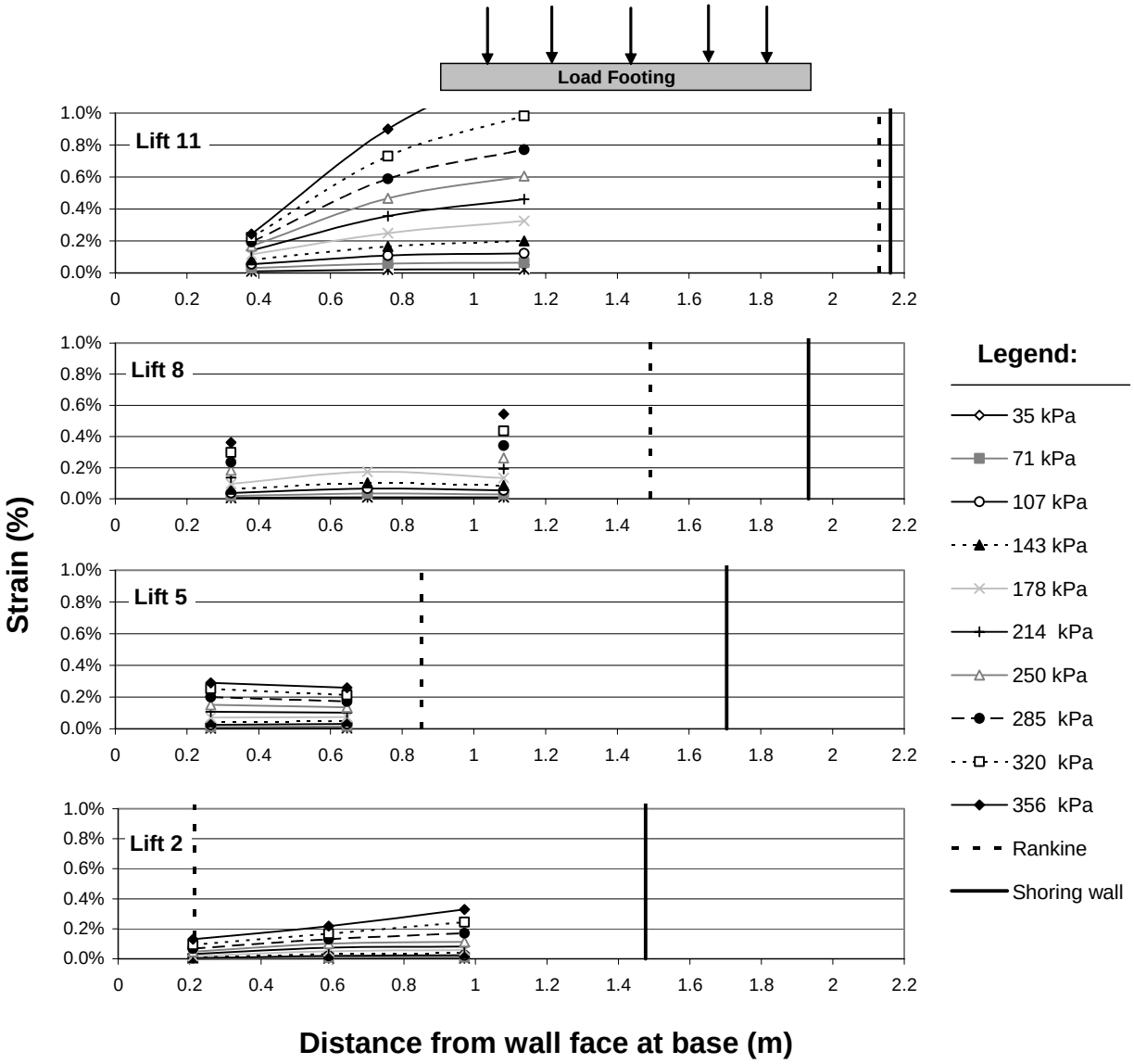


**Figure 63. Graph. Strain measurements in geogrid, unconnected wall system.**

Strain gages were installed on geogrid reinforcements for lifts 2, 5, 8, and 11 as the wall was constructed. Figures 62 and 63 illustrate the location of the shoring wall interface in relation to the strain gage locations, as well as the location of the theoretical Rankine failure surface based on a soil friction angle of 40 degrees. Some of the strain gages failed during load testing, as illustrated by discontinuous strain measurements. The measured strain in the geogrid increased with increasing elevation of the retaining wall and with increasing surcharge load, as illustrated in figure 64, which suggests that the reinforcements are fully engaged. Little difference was noted between the measured strain in the connected versus the unconnected wall systems. Measured strain generally corresponded to less than 1 percent which is well within the serviceability limits of the geogrid. The measured strain in each geogrid layer generally increased with distance from the wall face. However, strain gages installed on the fifth lift in the connected wall system

show the highest strain nearest to the wall face. Failure of one strain gage installed on lift five of the unconnected wall system prevented evaluation of a similar result. Peaks in the geogrid strain that might indicate a well developed shear zone were generally not detected. However, placement of the strain gages close to the MSE wall facing may not have allowed for the maximum geogrid strains to be captured.

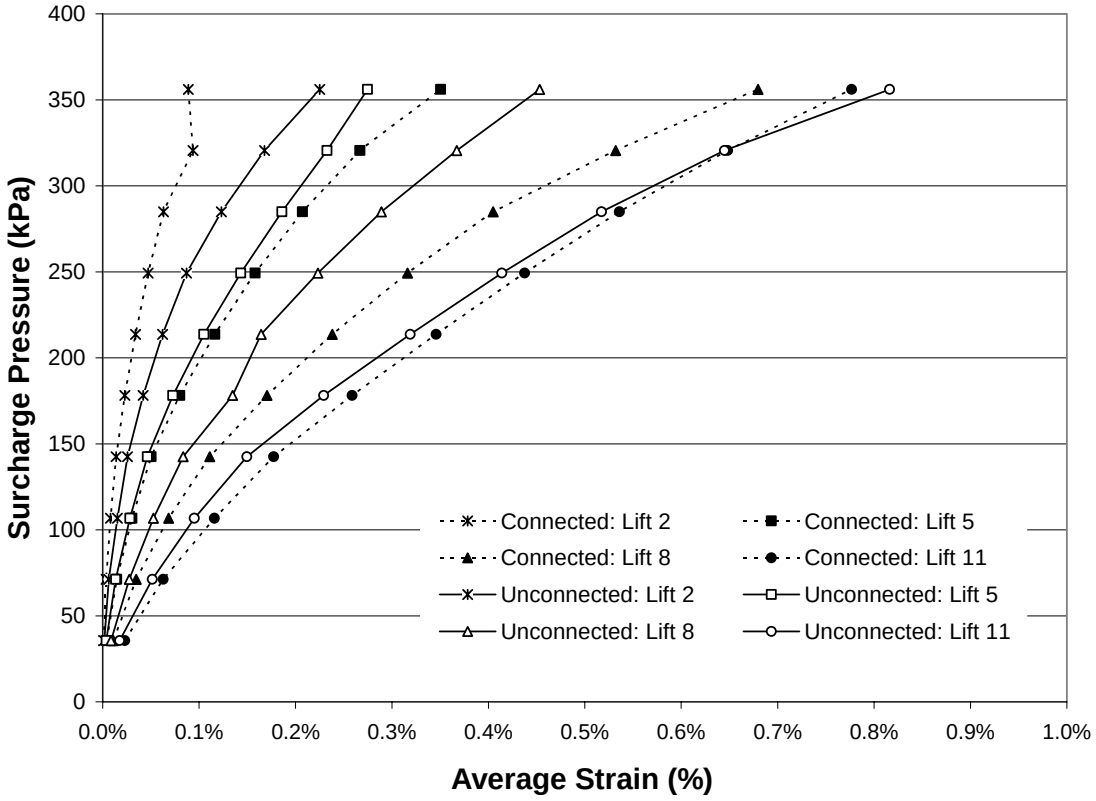


**Figure 64. Graph. Average measured strain versus applied surcharge pressure.**

### C.6.3 Pressure Cells

Horizontal and lateral vibrating wire earth pressure cells manufactured by Geokon were installed along each of the instrumented sections. Horizontal earth pressure cells were used to measure vertical stress as a function of overburden and applied load on the footing. Lateral earth pressure cells were used to measure lateral earth pressures at the back of the reinforced MSE mass.

The earth pressure cells consist of two circular stainless steel plates welded together around their periphery and spaced apart by a narrow cavity filled with de-aired oil. Increases in the earth pressure squeeze the two plates together causing an increase in the fluid pressure inside the cell. The vibrating wire pressure transducer converts this pressure into an electric signal which is transmitted at a frequency via a cable to the readout location. The standard model 4800 earth pressure cell was used to measure vertical earth pressures. The model 4810 earth pressure cell, which is designed to measure contact pressures on the surface of concrete or steel structures, has a thicker back plate to minimize point loading effects and was used to measure lateral earth pressures adjacent to the shoring wall. The cells were mounted on the battered shoring wall, resulting in measured lateral pressures that include a small component of vertical pressure.

### *Lateral Earth Pressure Cells*

Figure 65 compares the lateral earth pressure measurements for the connected and unconnected wall systems. The theoretical Rankine active earth pressures at zero surcharge and at the maximum surcharge loadings are plotted with the measured lateral earth pressures for comparison. The theoretical Rankine active lateral earth pressure ($\sigma_h$) was calculated as:

$$\sigma_h = \gamma H K_a + q K_a \qquad \textbf{Equation C.1}$$

where $\gamma$ is the unit weight of soil, $H$ is the wall height, $K_a$ is the active earth pressure coefficient, and $q$ is the surcharge loading. For the field-scale test wall, $K_a$ was calculated as 0.22 assuming a soil friction angle of 40 degrees. The theoretical Rankine active earth pressure curve at the maximum surcharge plotted in figure 65 was reduced assuming 35 percent coverage of the load footing.

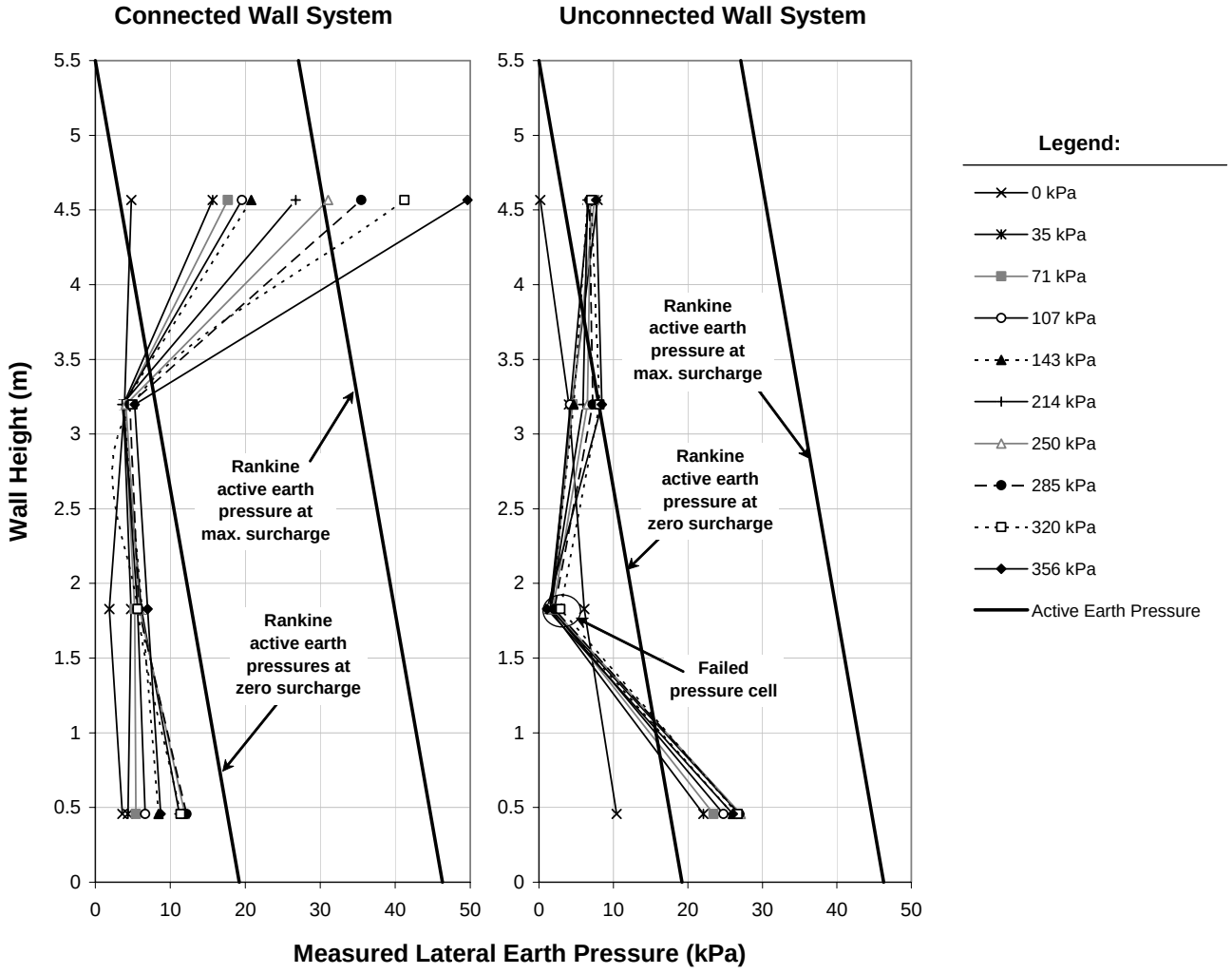


**Figure 65. Graph. Measured lateral earth pressures for the connected and unconnected wall systems.**

The measured lateral earth pressures generally increased with increasing surcharge load for both wall types. With the exception of the uppermost pressure cell for the connected wall system, the measured lateral earth pressures are generally less than the zero surcharge Rankine active earth pressures for both the connected and unconnected wall systems. The uppermost vertical pressure cell installed in the connected wall system recorded higher lateral earth pressures than all other cells. However, the measured lateral pressure remained considerably less than the estimated active earth pressures at representative surcharge loads.

For the connected wall system, the measured lateral earth pressures for the lower three cells are nominally less and parallel to the estimated active earth pressure distribution at zero surcharge. For the unconnected wall system, the pressure cell located approximately 1.8 meters above the base of the wall appears to have failed prior to load testing with negligible pressures measured at loading increments of 35 kPa to 356 kPa. With the exception of this pressure cell, the measured lateral earth pressures at all surcharge loads in the unconnected wall system generally approximate the estimated Rankine active earth pressure distribution at zero surcharge. The measured lateral pressures prior to load testing (at zero surcharge) were approximately 50 to 60 percent of the theoretical Rankine active earth pressure for the unconnected wall system; at larger surcharges, this ratio becomes inconsistent and may be strain dependent. The measured lateral pressures for the connected wall system did not parallel the theoretical Rankine active earth pressure.

Between the lateral pressure measurements for the two wall systems, the most significant difference occurs at the uppermost pressure cell. The lateral earth pressures at the uppermost pressure cell are relatively low for the unconnected wall system and significantly higher than the measurements at lower elevations for the connected wall system. Because the unconnected wall system was not tied to the shoring wall, the low lateral earth pressure measurements at the uppermost pressure cell may be due to development of a tension crack near the top of the wall. Conversely, the connected wall system which was tied to the shoring wall at each geogrid elevation exhibited considerably higher lateral pressures near the top of the wall. This appeared to be directly affected by the applied surcharge loading (i.e., increased lateral earth pressures with increased surcharge loading). The reduced lateral pressures measured at the top of the wall for the unconnected system increase the potential for tension crack development, further supporting extension of the upper MSE reinforcements over the shoring wall interface, as discussed in section 3.3.2.

### *Horizontal Earth Pressure Cells*

Figure 66 compares the vertical pressure measurements for the connected and unconnected wall systems, measured using the horizontal earth pressure cells. As expected, the measured vertical pressures under loading exceed the calculated overburden surcharge pressure. The measured vertical pressure at no surcharge corresponds very well to the theoretical curve, confirming that calculation of overburden pressures using the unit weight of the soil multiplied by the wall height ($\gamma H$) are appropriate for this wall. The shape of the measured vertical pressure distribution is approximately the same for the connected and unconnected wall systems.

The theoretical pressure distributions for the 35 kPa (89 kN) and 356 kPa (890 kN) surcharge load increments were evaluated using the 2:1 pyramidal distribution method (per figure 18, chapter 5), plotted on figure 66. At relatively low surcharge pressures, similar to those that would be encountered in practice, the 2:1 method appears to provide a reasonable estimate of the vertical pressures at depth from applied surcharge loading. However, at high loads (i.e., 356 kPa), the 2:1 method appears to underpredict the vertical stress in the MSE wall.

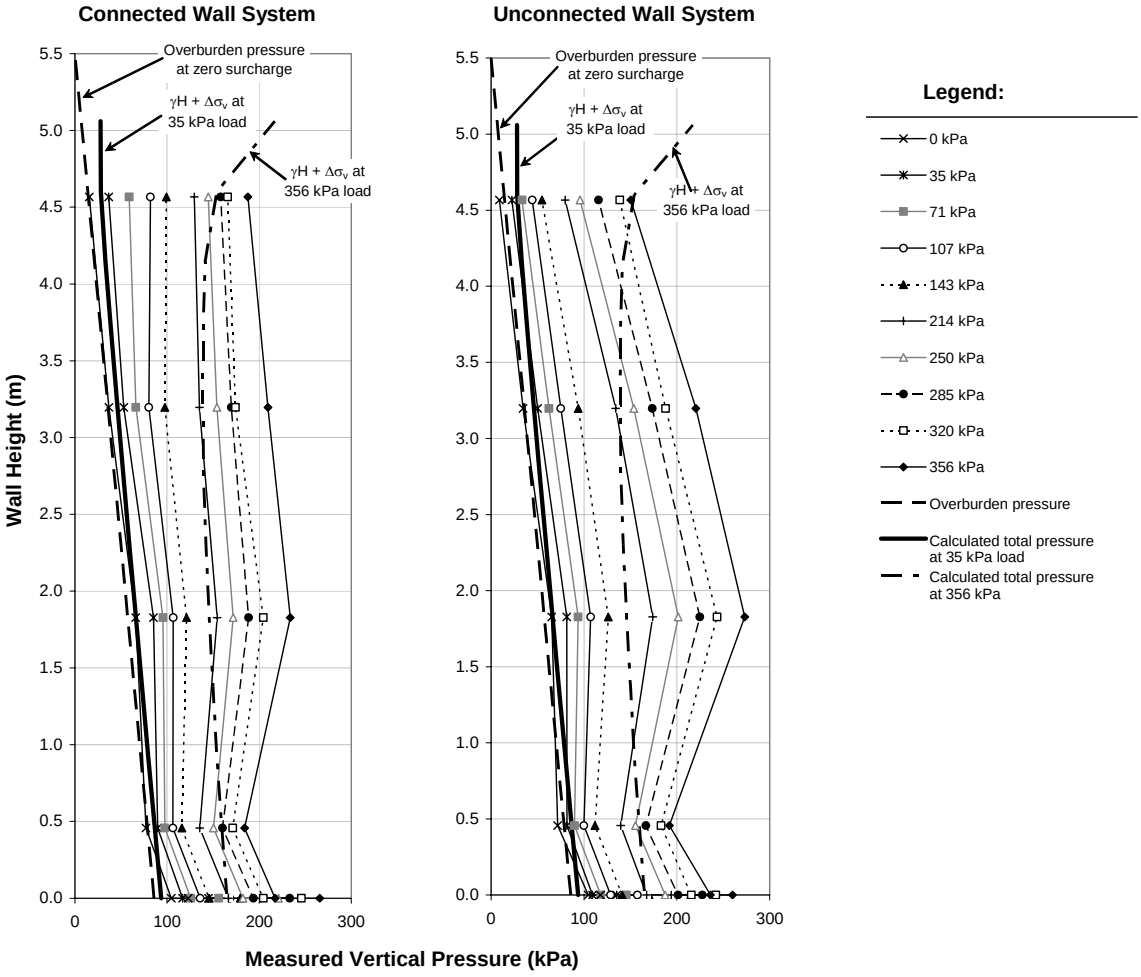


**Figure 66. Graph. Measured vertical pressures for the connected and unconnected wall systems.**

Figure 67 compares the measured vertical pressures versus the applied surcharge loading pressures. Due to the dimensions of the load footings, loads were applied to approximately 35 percent of the total top of wall area. As such, the measured vertical earth pressures are generally less than the applied vertical surcharge load, and generally on the order of 25 to 50 percent. In the upper half of the wall, a greater percentage of the applied load is observed (approximately 50 percent). In the lower two lifts of the wall, the measured load is approximately 25 percent of the applied load.

At the base of the wall, the vertical pressures measured at pressure cell "A" nearest to the shoring wall were approximately 20 percent less than the vertical pressures measured at the adjacent "B" pressure cells, which were located nearer to the wall facing. This infers that the shoring wall in essence absorbed a portion of the vertical stress, which may be indicative of arching in the vicinity of the shoring wall near the base of the wall.

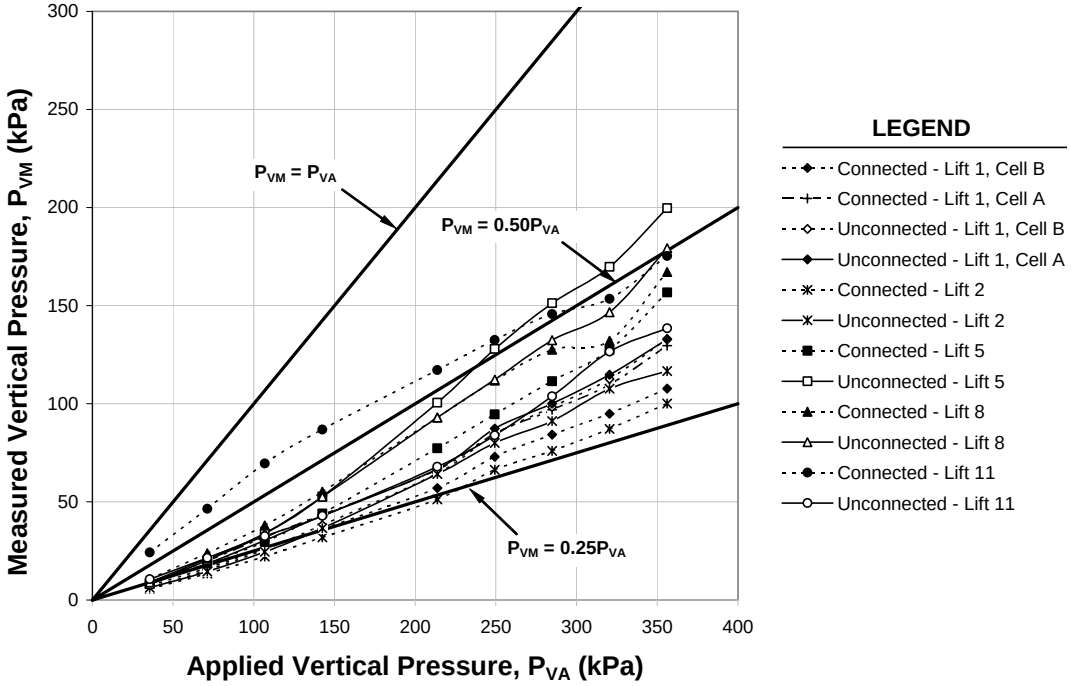


**Figure 67. Graph. Measured versus applied vertical pressures excluding overburden.**

The measured lateral earth pressures at each loading increment were divided by the measured vertical earth pressures to estimate the horizontal force coefficient, *K*, presented in figure 68. Recall that the vertical earth pressure cells were placed adjacent to the shoring wall, resulting in "lateral" earth pressure measurements that include a small degree of vertical pressures. The horizontal force coefficient ranged from less than 0.1 to about 0.4, with a calculated active earth pressure coefficient, $K_a$, of approximately 0.22. For use of geosynthetic reinforcements, Lawson and Lee concluded that $K$ is less than $K_a$ for aspect ratios less than 0.5.[5] This appears to generally be the case for the field-scale test wall which was constructed with an aspect ratio varying from 0.25 at the base to 0.39 at the top of the wall.

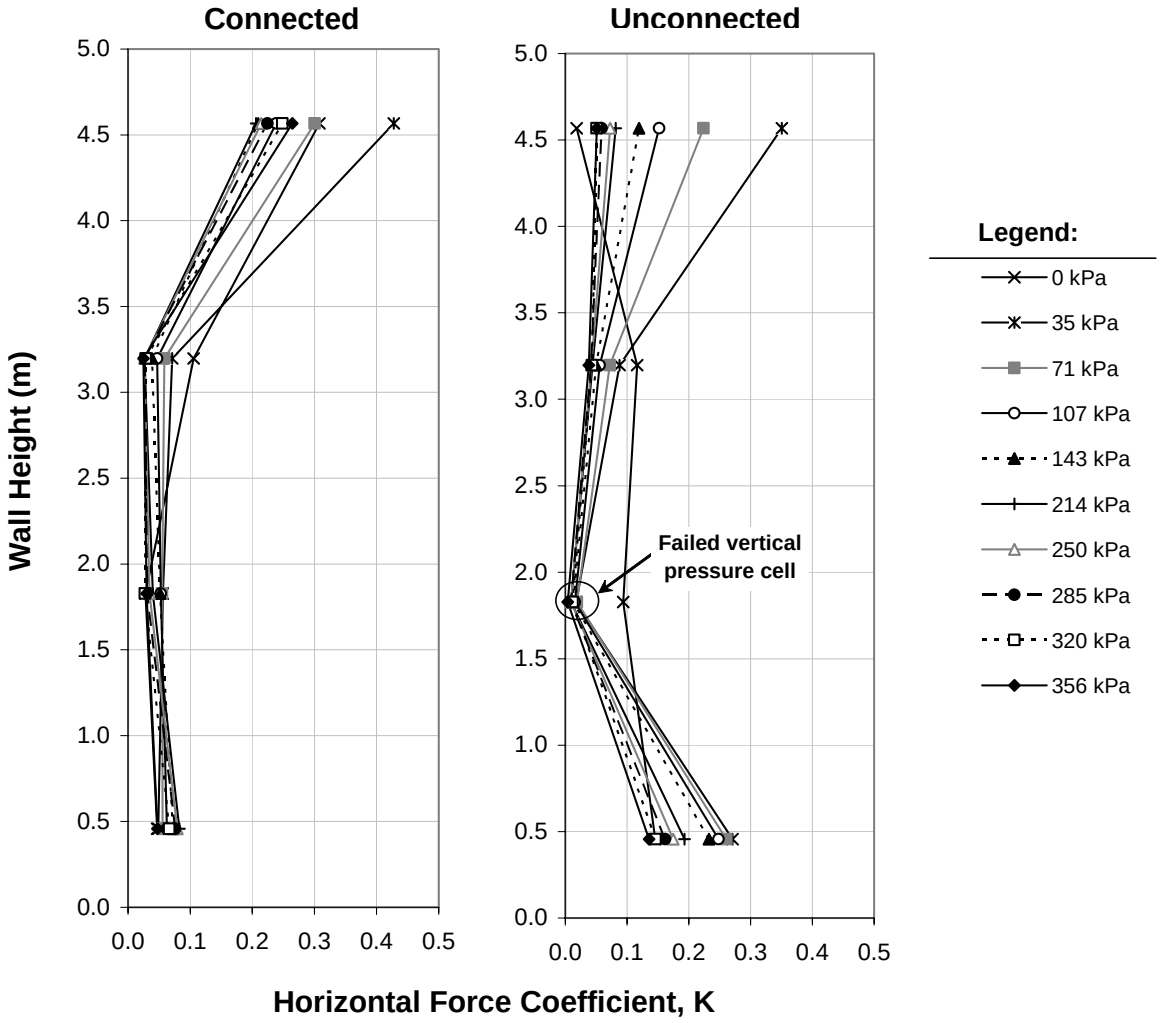


**Figure 68. Graph. Calculated lateral earth pressure coefficient.**

### C.6.4 Inclinometer Measurements

A total of four inclinometers were installed as part of the instrumentation program. Two of the inclinometers were installed to measure horizontal deflection of the MSE wall face, and two were installed to monitor horizontal deflection of the shoring wall, if any.

The inclinometers were measured by TFHRC assuming the top of each inclinometer casing as a fixed point. Figure 69 presents the measured cumulative displacement of the inclinometers installed at the face of the MSE wall for the connected and unconnected wall systems. The measured cumulative displacements of the connected and unconnected portions of the MSE wall were similar, indicating a maximum horizontal displacement with respect to the top of the wall on the order of 8 mm outward.

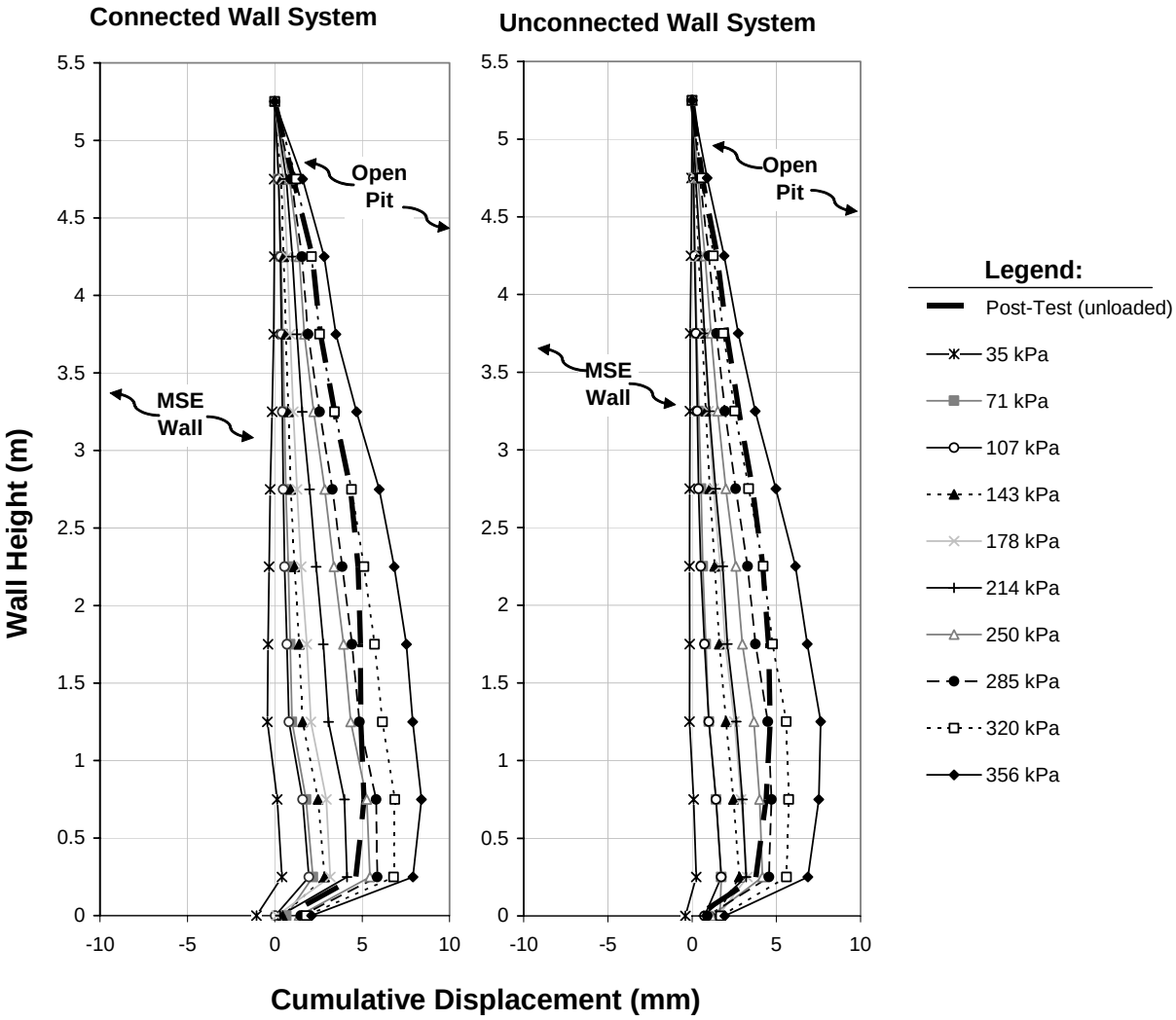


**Figure 69. Graph. Measured cumulative displacement of MSE wall face.**

Figure 70 presents the measured cumulative displacement of the shoring wall face. As demonstrated by the inclinometer measurements, the shoring wall exhibited negligible deflection, except perhaps a few millimeters of movement, increasing towards the bottom. Note that the measurement at 320 kPa for the connected wall section appears to be erroneous.

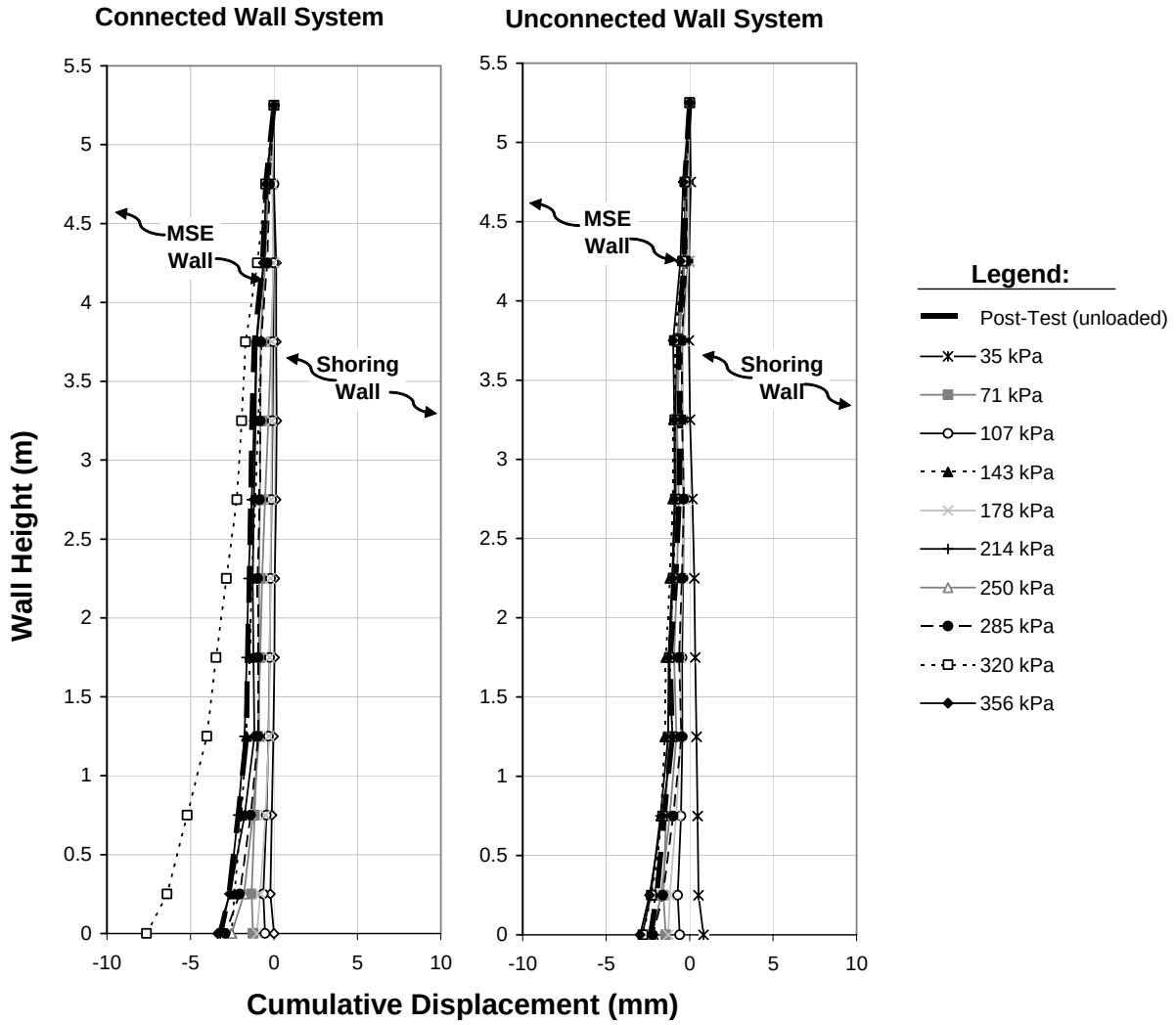


**Figure 70. Graph. Measured cumulative displacement of shoring wall.**

### C.6.5 Survey Measurements

Vertical and horizontal deflections of the load footing were measured using total station, level, and linear variable displacement transducers (LVDT). The total station enabled measurements of both vertical settlement and horizontal displacements, illustrated in figures 71 and 72, respectively. Connection of the shoring wall to the MSE wall did not appear to have a significant impact on footing settlement, with the measured maximum vertical settlement of the load footings for both the connected and unconnected systems on the order of 16 mm. Measured horizontal displacement of the load footings ranged from 4 to 9 mm for the connected wall system, and from 8 to 13 mm for the unconnected wall system. Because the measured horizontal displacement of the unconnected wall was greater than that of the connected wall, extension of the upper MSE reinforcements beyond the limits of the shoring wall is further recommended to decrease deformation for an unconnected wall, as discussed in section 3.3.2. The maximum

horizontal displacement of the load footing for the connected wall system was measured for the portion of the footing closest to the unconnected wall section, with larger horizontal displacements measured for the unconnected wall section.

Settlement measurements obtained from the total station were compared to settlement measurements obtained using the level, illustrated in figure 73. The level measurements compared well with the total station data, verifying the total station data.

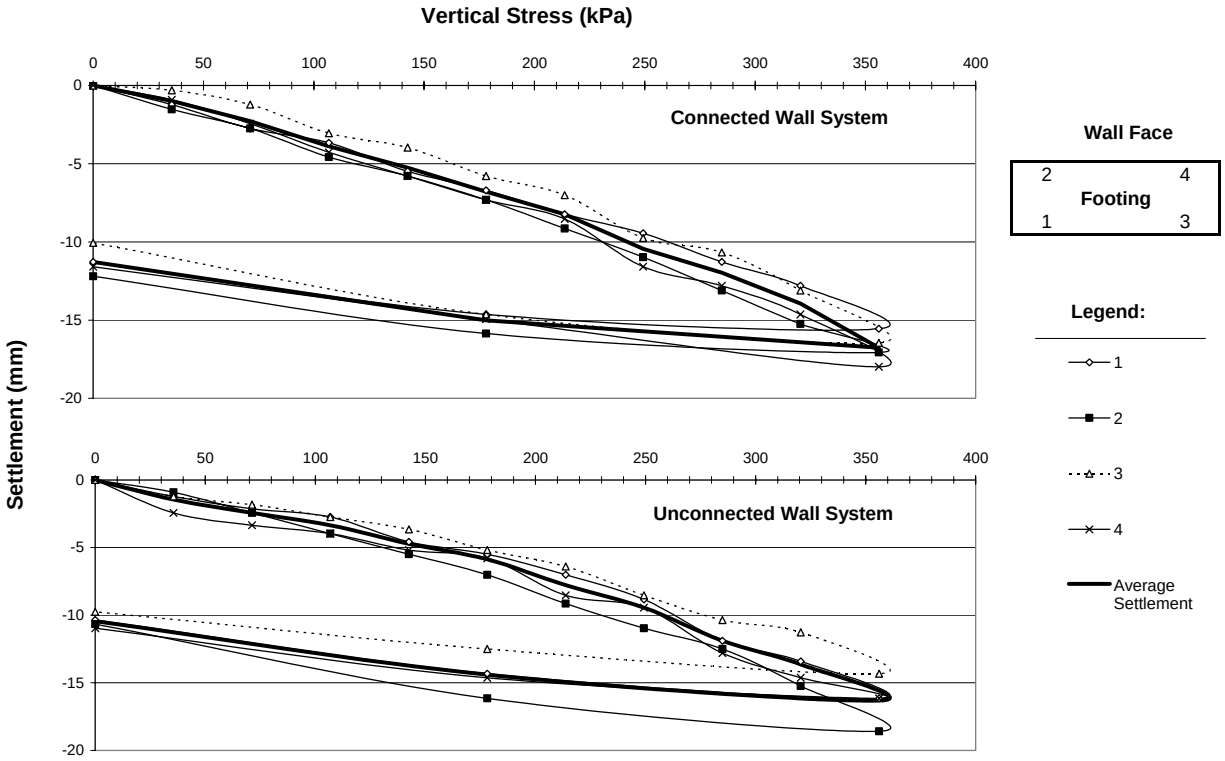


**Figure 71. Graph. Measured settlement of load footings using total station.**

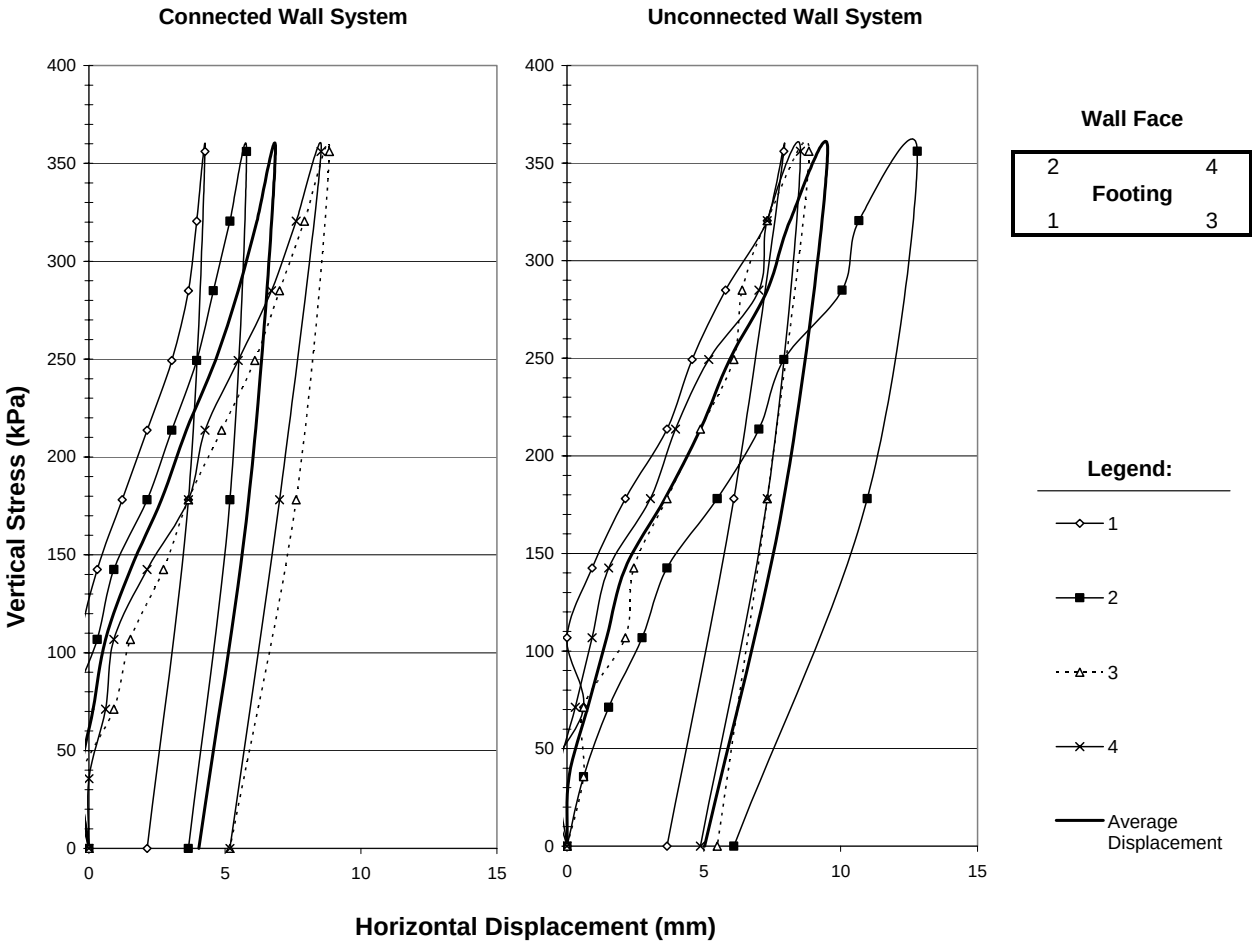


**Figure 72. Graph. Measured horizontal displacement of load footings using total station.**

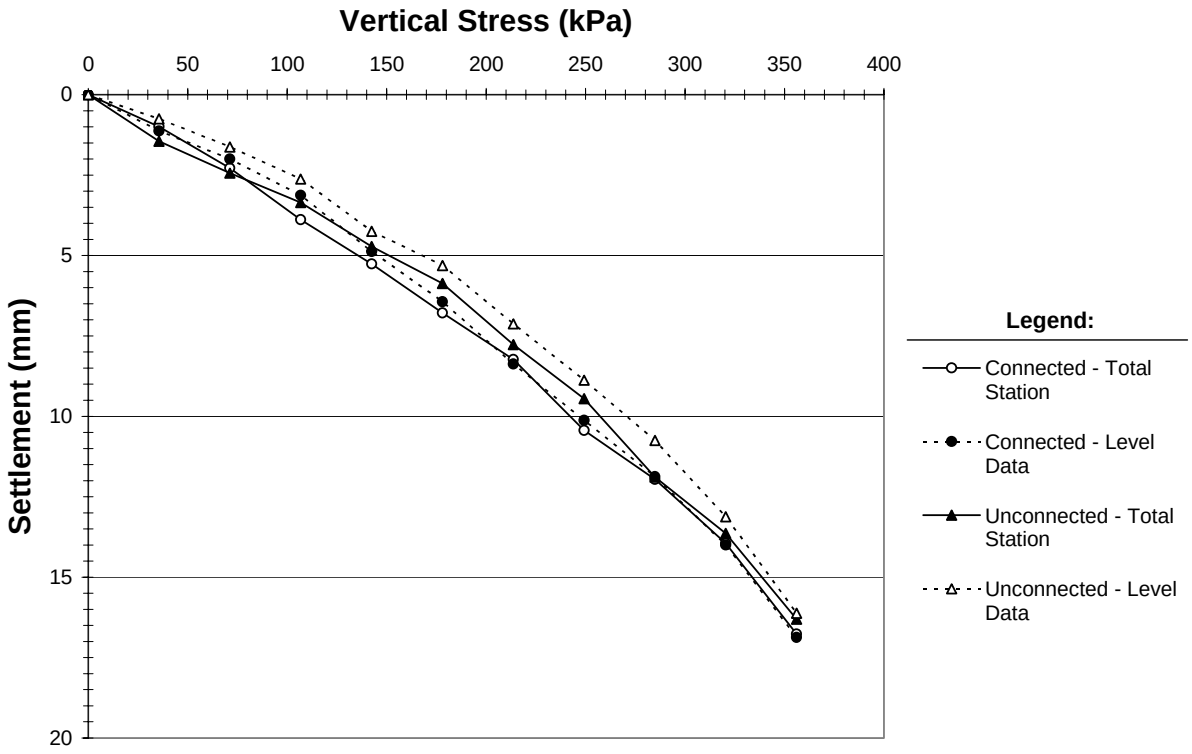


**Figure 73. Graph. Comparison of settlement measurements obtained using total station and level.**

### C.6.6 LVDT Measurements

Linear variable displacement transducers (LVDT) manufactured by Solartron Metrology were used to measure vertical displacement at each corner of the footings. Direct current (DC) sprung armature type LVDTs were used to measure footing displacement.

Figure 74 presents the average vertical settlement of the load footings measured using LVDT. The connected wall system appeared to settle slightly more than the unconnected wall section at each load increment, with a maximum measured average settlement of approximately 18 mm compared to 17 mm. The LVDT measurements were similar to the total station vertical displacement measurements which resulted in approximately 16 mm of settlement for both wall sections.

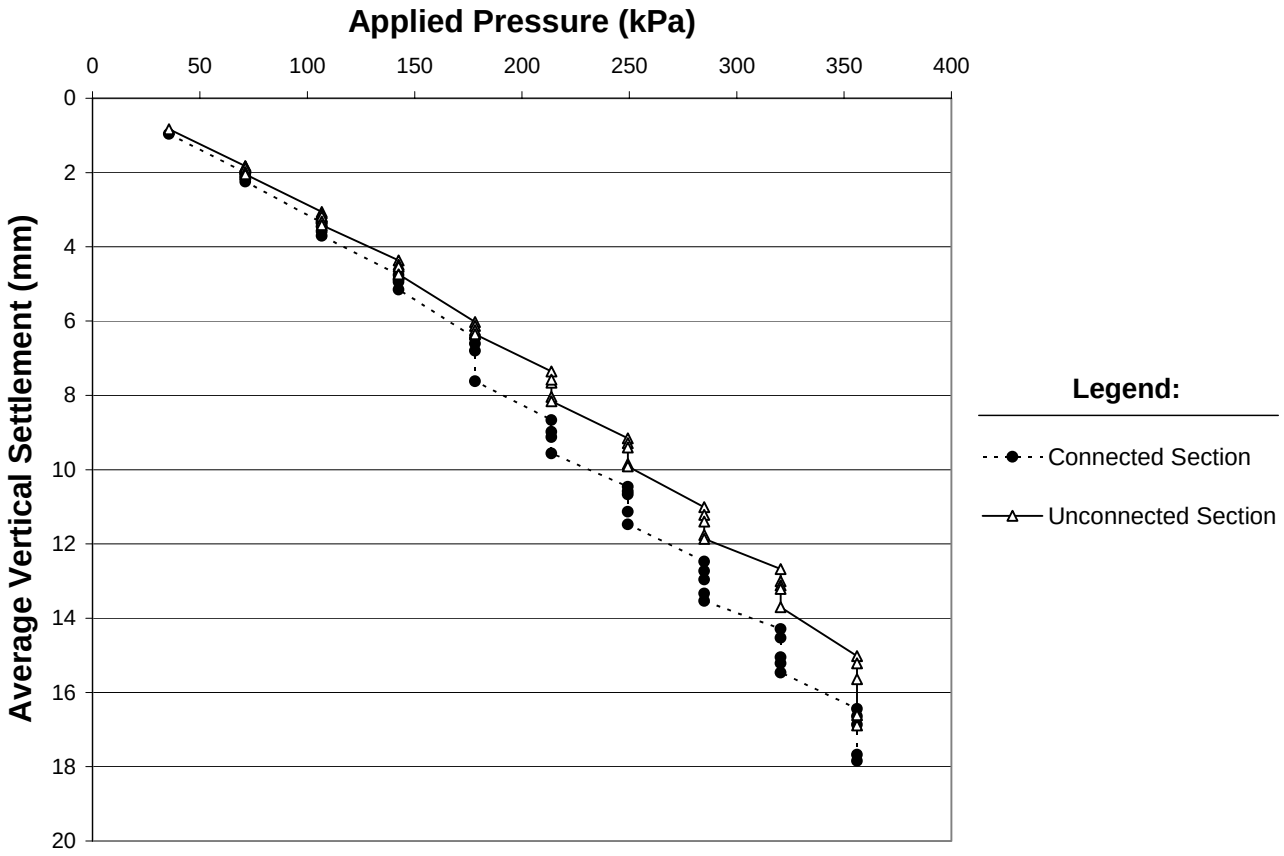


**Figure 74. Graph. Average vertical settlement of load footings measured using LVDT.**

### C.6.7 Potentiometer Measurements

Lateral displacement of the MSE wall face was measured using potentiometers. The potentiometers were firmly mounted on H-type steel beams using C-clamps. The extended stainless steel cable was connected and bolted onto the face of the wire basket near the center-height of the facing element. Potentiometers were installed at five levels near the top, middle and bottom of each wall section, corresponding to lifts 2, 5, 8, 11, and 12 (from bottom to top). Two instrumented sections were selected: one near the center of the connected wall system, and one near the center of the unconnected wall system.

The purpose of the potentiometers was to measure lateral deformation of the MSE wall. Figure 75 illustrates the potentiometer measurements for the connected and unconnected wall systems. Data is not shown for potentiometers located on lifts 11 and 12 for the connected wall system and lifts 2, 5, 8, and 12 for the unconnected wall system as these instruments produced erratic data. Measured lateral displacement of the MSE wall face ranged from less than 1 mm near the base of the wall to 18 mm near the center of the wall for the connected wall system. Only one potentiometer on the unconnected wall system produced reasonable results, indicating about 10 mm of lateral displacement near the top of the wall.

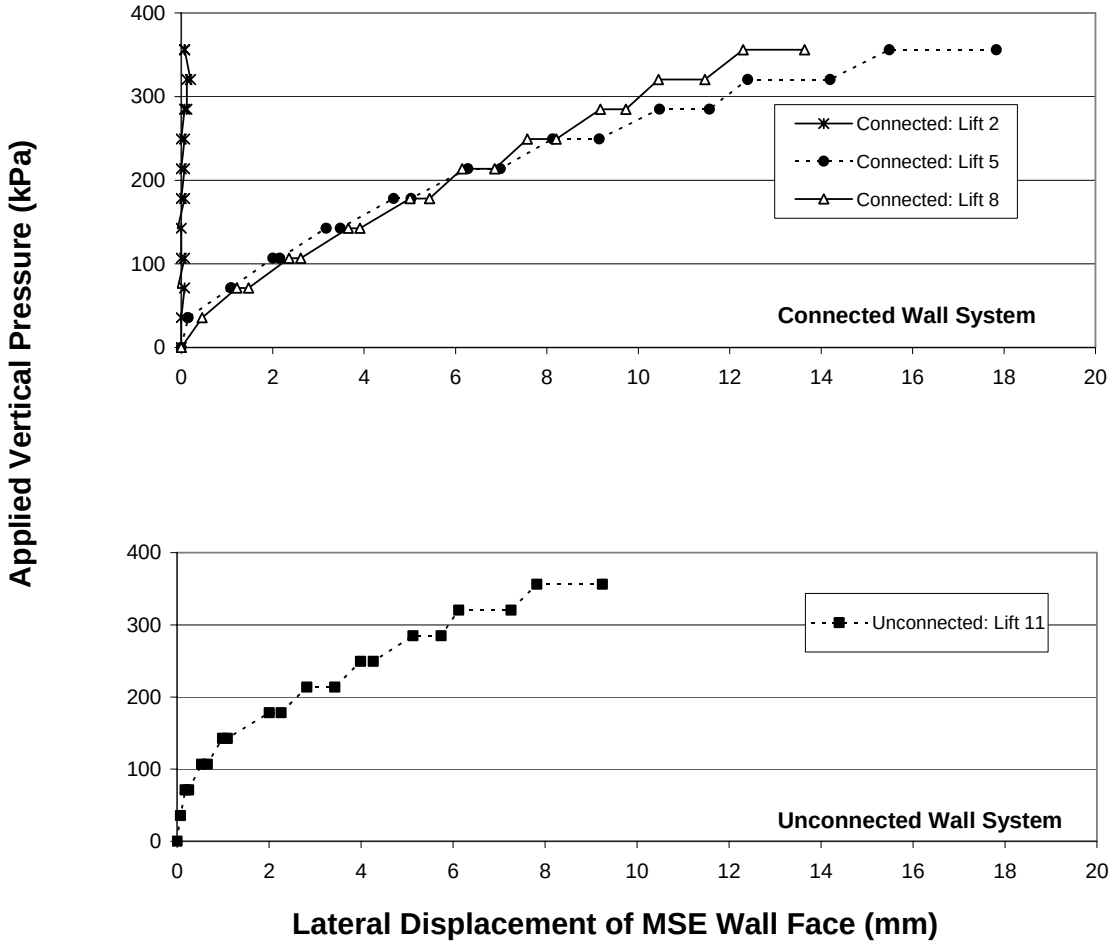


**Figure 75. Graph. Potentiometer measurements for the connected and unconnected wall systems.**

Based on visual observations of the MSE wall face during load testing, it appeared that the wall face rotated and shifted slightly during loading which may have contributed to erroneous potentiometer measurements. Observations of wall construction revealed that generally no transverse bars were present in the geogrid wrap extending behind the face of the wall. The lack of transverse bars near the face of the wall appears to have been either a design oversight and not clearly spelled out in the construction specifications, or inadvertently omitted during construction. It is believed that this lack of facing reinforcement contributed to isolated deformations of the wall face, resulting in potentiometer data that do not reflect horizontal movement of the MSE mass. Therefore, potentiometer data were not used for analysis of wall deformation.

## C.7 INSTRUMENTATION SUMMARY

As demonstrated by strain gages installed at various geogrid levels within the MSE soil mass, the measured strain in the geogrid reinforcements increased with increasing elevation of the

retaining wall and with increasing surcharge pressure. Strain was generally less than one percent which is well within the serviceability limits of the geogrid. Similar behavior was noted for the connected and unconnected wall systems.

Lateral earth pressure measurements recorded at the back of the MSE mass adjacent to the shoring wall generally show lateral earth pressures less than or equal to the theoretical zero surcharge Rankine active earth pressures for both the connected and unconnected wall systems. Measured lateral earth pressures are relatively low for the uppermost pressure cell installed in the unconnected wall section, possibly due to development of a tension crack. However, the measured lateral earth pressures for the uppermost pressure cell installed in the connected wall section are significantly higher, and appear to be directly affected by the applied surcharge loading.

Measured vertical earth pressures were similar for the two wall systems with the vertical stress at zero surcharge corresponding to $\gamma H$, and vertical earth pressures increasing along with the surcharge level. Also, a decrease in vertical pressure near the base of the wall was observed. The vertical pressures measured at the base of the wall were observed to be approximately 20 percent higher for the pressure cell located closer to the face of the MSE wall than the pressure cell located closer to the shoring interface, possibly as a result of arching. The measured vertical earth pressure increase was less than the applied vertical surcharge load due to the fact that the load footings covered only approximately 35 percent of the surface area. In the upper half of the wall, the measured load is approximately 50 percent of the applied load, and in the lower half of the wall, the measured load is approximately 25 percent of the applied load.

Inclinometers installed at the face of the MSE wall show no significant variation in cumulative displacement between the connected and unconnected wall sections, with a maximum cumulative displacement on the order of 8 mm with respect to the top of the wall. Inclinometers installed at the shoring interface measured negligible movement.

Survey measurements indicated that settlement of the unconnected and connected wall system footings were essentially the same. However, horizontal displacement of the load footing for the unconnected wall system was nominally larger than that measured for the connected wall system. The variation in horizontal displacement may be due to development of a tension crack behind the MSE mass in the unconnected wall system. Potentiometer data were considered nonconclusive.

## C.8 COMPARISON OF CENTRIFUGE AND FIELD-SCALE MODELING

The following components differed between the centrifuge model and the field-scale load test:

- The equivalent width of the footing used to apply load to the top of the centrifuge model was 1.4 m, while the concrete footing used for load testing of the field-scale test was 1 m.

- The centrifuge model was loaded to a maximum equivalent footing pressure of 239 kPa. The field-scale test wall was loaded to a maximum footing pressure of 356 kPa. Neither model exhibited failure at the maximum test load.

- The centrifuge prototype was modeled for the wall section without mechanical connection to the shoring wall (i.e., unconnected system).

- Reinforcing elements installed in the centrifuge prototype had a tensile strength of 18 kN/m, which is approximately 35 percent of the tensile strength of the geogrid used to construct the field-scale test wall (i.e., 52 kN/m).

- Two additional reinforcement layers were installed near the top of the field-scale test wall to prevent bearing capacity failure of the footing at the surface. The centrifuge test wall did not have the additional reinforcing layers and appeared to fail in bearing capacity directly beneath the load footing.

After the centrifuge model was loaded to 239 kPa without failure, the acceleration level was increased until failure occurred. The centrifuge model prototype proceeded to fail at an acceleration of 32*g*, which is equivalent to a prototype height of 11.0 m. At this increased acceleration level, the reinforcement vertical spacing corresponded to approximately 0.9 m. The field-scale test wall was constructed to a maximum height of approximately 5.5 m with a reinforcement vertical spacing of approximately 0.46 m.

Bonded resistance strain gages were installed in the field-scale test model to enable evaluation of local stress and strain distribution in the geogrid reinforcing elements and identify areas of maximum stress. Strain gages were installed on four layers of geogrid in the field-scale test wall near the top, middle and bottom of the wall section, corresponding to lifts 2, 5, 8, and 11 (from bottom to top), and near the front, middle and back of each reinforcing element (i.e., 0.20 m, 0.57 m, and 0.95 m from the face of the MSE wall). Figure 63 presented the strain measurements obtained from gages installed in the unconnected wall system, illustrating also the location of the shoring wall interface in relation to the strain gage locations as well as the location of the theoretical Rankine failure surface based on a soil friction angle of 40 degrees. Some of the strain gages failed during load testing, as illustrated by discontinuous strain measurements, as shown on figure 63. However, one strain gage failed prior to load testing and produced no data.

The locations of strain gages installed in the field-scale test model were compared to digital imaging locations of torn reinforcement from the failed centrifuge model, as illustrated in figure 76. The location of the theoretical active failure wedge is illustrated based on an estimated soil friction angle of 40 degrees. Failure of the centrifuge model appears to have occurred relatively close to the active failure wedge for the lower half of the wall. In the upper half of the wall, an opposing active failure wedge appears to have developed as a result of bearing capacity failure of the soil beneath the load footing.

Based on the results of the centrifuge testing, the strain gages were generally located within the expected zone of highest strain on the geogrid. Results from the instrumented layers of geogrid from the field-scale test are compared to the centrifuge test results, as follows:

- Lift 11 – Based on centrifuge testing, the maximum strain was expected for the central strain gage. However, the maximum measured strain occurred for the strain gage located nearest the shoring wall.

- Lift 8 – Based on centrifuge testing, the maximum strain was expected for the strain gage located nearest the shoring wall. However, the central strain gage appears to correspond to the peak strain. Failure of this strain gage during load testing may further indicate that this gage exhibited the maximum strain.

- Lift 5 – Based on the results of centrifuge testing, the expected maximum strain would correspond to the location of the strain gage closest to the shoring wall. This particular strain gage failed prior to load testing.

- Lift 2 – The maximum strain measured during field testing was for the strain gage located closest to the shoring wall. Centrifuge testing generally produced failure through the wall face at a corresponding elevation.

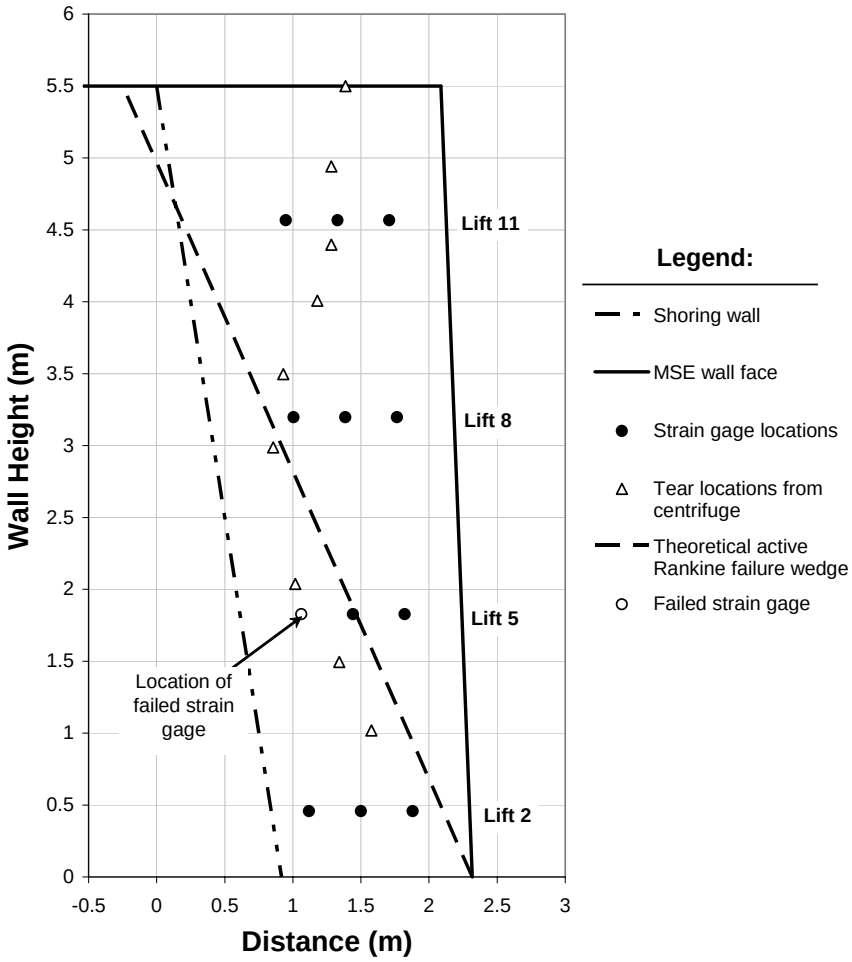


**Figure 76. Graph. Comparison of centrifuge reinforcement tears to field-scale test wall strain gage locations.**

Trend lines were drawn through the reinforcement tears developed during centrifuge testing and compared to the theoretical active failure wedge based on a soil friction angle of 40 degrees, illustrated in figure 77.

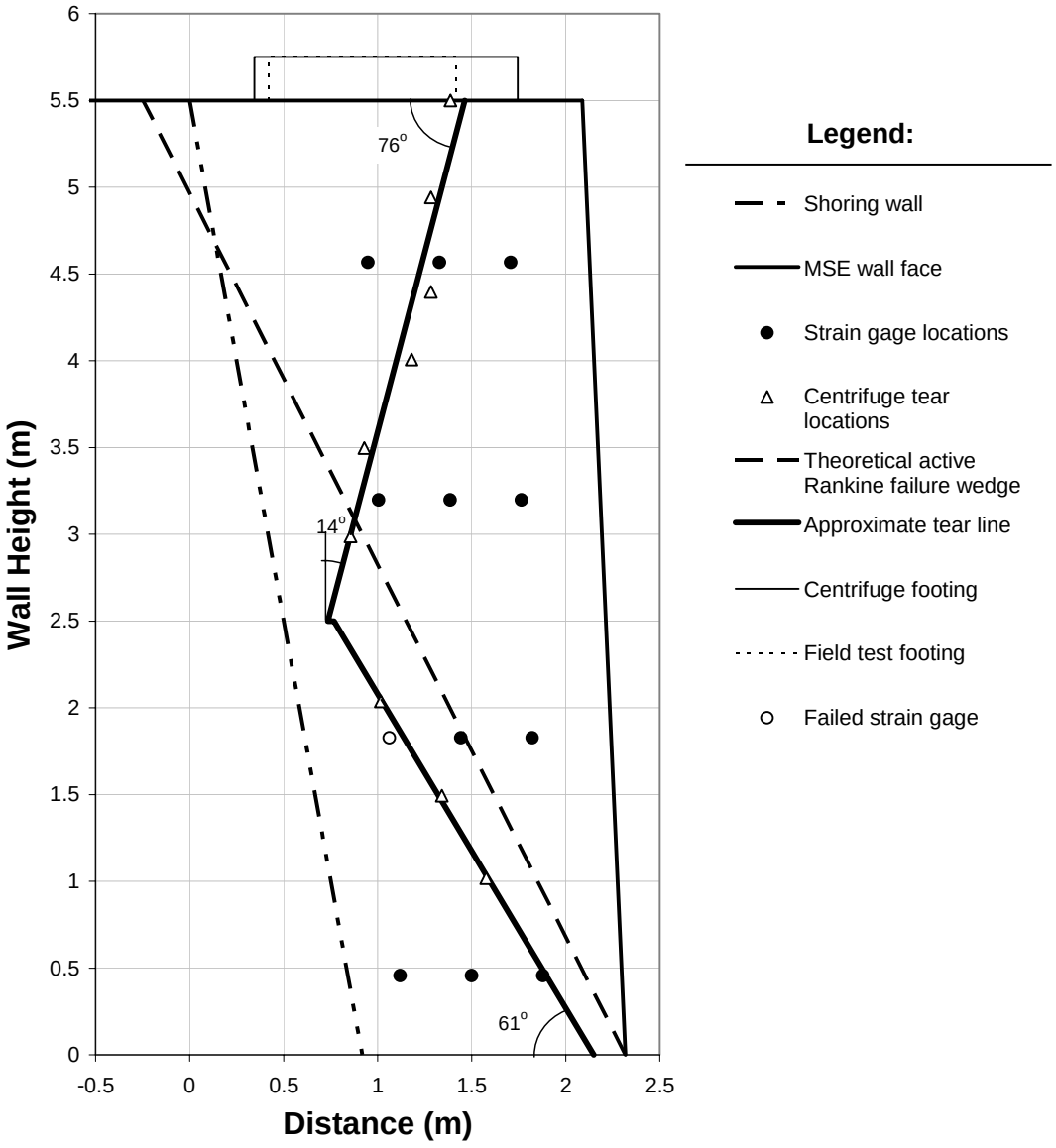


**Figure 77. Graph. Comparison of theoretical active failure wedge to actual failure geometry.**

The lower portion of the centrifuge test wall exhibited failure which approximately paralleled the active failure wedge theory, failing with a base angle of 61 degrees as compared to the theoretical base angle of 65 degrees. The centrifuge model did not appear to fail out the toe point, but instead nominally back into the MSE wall reinforced zone. The upper portion of the

centrifuge model exhibited a wedge failure at an approximately twice as steep of angle (14 degrees as compared to 29 degrees) than a corresponding active failure wedge.

The locations of the load footings for centrifuge and field-scale testing are shown on figure 77. The failure surface for the upper portion of the wall obtained from centrifuge testing approximates the active failure wedge from bearing capacity theory. The angle of the active bearing capacity failure surface measured from horizontal is generally assumed to be equal to the soil friction angle.[63] However, the failure surface is inclined at approximately 76 degrees to horizontal compared to an estimated soil friction angle of 40 degrees. This may be attributed to the increased frictional resistance of the soil due to installation of MSE reinforcing elements.

## C.9 FACTOR OF SAFETY CALCULATION

The factor of safety of the field-scale test wall with regard to internal stability was calculated under the maximum test pressure of 356 kPa using the design procedure outlined in section 5.3 (chapter 5). The calculations are presented in this section.

### C.9.1 Internal Stability Calculation

This section presents a check on the internal stability design of the unconnected portion of the test wall at the maximum footing load of 890 kN (356 kPa).

***Step 1 - Identify MSE wall type, geometry, and loading conditions.***

The details of the wall design and loading conditions are summarized as follows:

- Because the test wall was constructed for research purposes only, no embedment was constructed at the toe of the test wall. Therefore, the design height, $H_d$, of 5.5 m is equivalent to the overall height.

- MSE facing elements consisted of Tensar® welded wire facing units having a unit height of approximately 0.46 m. Given the facing unit size, a vertical spacing of 0.46 m was used, allowing for one reinforcement per facing unit.

- The MSE wall was constructed with a facing batter of 1H:24V and the shoring wall with a batter of 1H:6V.

- MSE reinforcements ranged in length, increasing from 1.4 m at the base to approximately 2.1 m near the top of the wall.

- MSE reinforcements consisted of Tensar® UX1500MSE geogrid with a reported allowable tensile strength of 52 kN/m at 5 percent strain, and an ultimate tensile strength of 114 kN/m. Geogrids were installed with 100 percent coverage.

- Because the test load was concentrated and applied to a footing, the test load is considered a concentrated vertical load as opposed to a surcharge load. The vertical stress at each

reinforcement level is calculated by applying the maximum test load of 890 kN to a footing with dimensions of 1 m by 2.5 m, per figure 78.

***Step 2 – Estimate the location of the critical failure surface.***

The critical failure surface may be approximated using the theoretical active failure surface within the reinforced soil mass at the base of the wall, with the remaining portion intersecting the interface of the shoring and MSE wall components, per figure 14 in chapter 5 for extensible reinforcements. In order to estimate the location of the failure surface, engineering properties of the reinforced backfill must be established, as follows:

- Based on results of direct shear testing, an effective friction angle, $\phi'$, of 40$^o$ was assumed for the reinforced fill. The test wall was constructed with a density of 102 to 105 percent of the maximum dry density determined using AASHTO T-99 ($\gamma_{max}$ = 15.3 kN/m$^3$). Therefore, assume a unit weight, $\gamma$, of 15.6 kN/m$^3$ for the reinforced backfill.

- For extensible reinforcements, $\psi = 45^o + \phi'/2 = 65^o$.

- The foundation of the test wall was assumed to be sufficiently competent, as the test wall was constructed inside a concrete pit having a concrete foundation. As such, the bearing capacity and settlement of the foundation was not evaluated.

***Step 3 – Calculate internal stability with respect to rupture of the reinforcements.***

The calculation for reinforcement rupture is as follows:

- Calculate the active earth pressure coefficient, $K_a$, using equation 1 in chapter 5 for MSE facing batters less than 8 degrees ($K_a$ = 0.217). For extensible reinforcements, the lateral stress ratio, $K_r/K_a$, is one, per figure 16 in chapter 5.

- At each reinforcement level, calculate the horizontal stress, $\sigma_h$, along the potential failure line from the weight of the reinforced fill, plus uniform surcharge loads, and concentrated surcharge loads ($\Delta\sigma_h$, $\Delta\sigma_v$) using equations 3 and 4 presented in chapter 5.

- Because the loading was applied to a footing, calculate the concentrated vertical stress, $\Delta\sigma_v$, at each reinforcement level using the 2:1 method (figure 18, chapter 5). Figure 78 illustrates calculation of $\Delta\sigma_v$ for the field-scale test wall geometry.

- Using the horizontal stress, $\sigma_h$, calculate the maximum tension per unit width of wall based on the vertical reinforcement spacing ($s_v$) of 0.46 m using equation 5 presented in chapter 5.

Figure 79 summarizes the reinforcement rupture calculations conducted for the test wall under the maximum test load. Based on the calculations presented in figure 79 for $T_i$ at each reinforcement level, the field-scale test wall was designed adequately for rupture as Tensar® UX1500MSE geogrid (which was used for wall construction) has a reported ultimate tensile

strength of 114 kN/m, which was higher than the calculated maximum tension of approximately 22 kN/m.

## CONCENTRATED VERTICAL LOAD CALCULATION

**Field-scale test wall:**

**CALCULATION OF VERTICAL STRESS DUE TO FOOTING:**

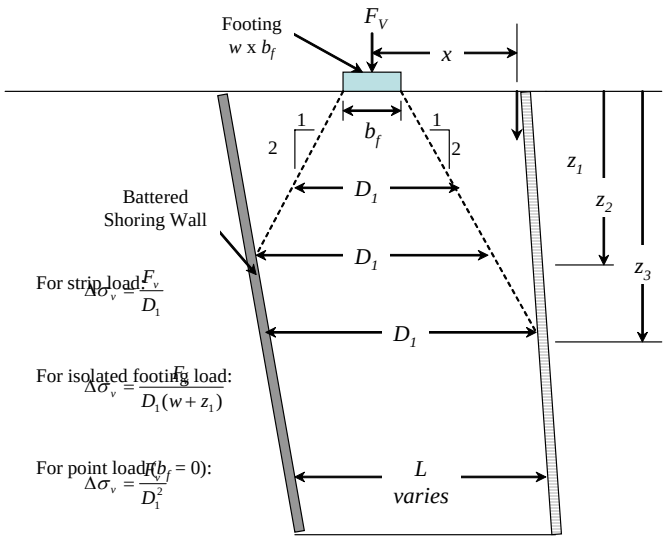


For $z_1 \le z_2$ : $D_1 = b_f + z_1$

For $z_3 > z_1 > z_2$ : $D_1 = \frac{b_f + z_1}{2} + x$

For $z_1 \ge z_3$ : $D_1 = L$

| Loading parameters: | | |
|---|---|---|
| Load, $F_v$: | 890 | kN |
| Footing length, w: | 2.5 | m |
| Footing width, $b_f$: | 1 | m |

| Calculated based on wall geometries: | | |
|---|---|---|
| $z_2$: | 0.63 | m |
| $z_3$: | 1.24 | m |
| x: | 0.92 | m |

| Footing load type: | Isolated |
|---|---|

Input Fields
Calculated Fields

***Calculation modified from Elias et al. (2) for SMSE walls.***

For the field-scale test wall, the shoring wall was battered at 1H:6V and the MSE face at 1H:24V. Lengths, L, calculated manually.

| Layer | $z_1$ (m) | L (m) | $D_1$ (m) | $\Delta\sigma_v$ (kPa) |
|---|---|---|---|---|
| 1 | 5.50 | 1.40 | 1.40 | 79.5 |
| 2 | 5.04 | 1.46 | 1.46 | 80.8 |
| 3 | 4.58 | 1.52 | 1.52 | 82.7 |
| 4 | 4.12 | 1.57 | 1.57 | 85.6 |
| 5 | 3.66 | 1.63 | 1.63 | 88.6 |
| 6 | 3.20 | 1.69 | 1.69 | 92.4 |
| 7 | 2.74 | 1.75 | 1.75 | 97.1 |
| 8 | 2.28 | 1.80 | 1.80 | 103.4 |
| 9 | 1.82 | 1.86 | 1.86 | 110.8 |
| 10 | 1.36 | 1.92 | 1.92 | 120.1 |
| 11 | 0.90 | 1.98 | 1.87 | 140.0 |
| 12 | 0.44 | 2.03 | 1.44 | 210.2 |

**Figure 78. Calculation. Calculation of vertical stress due to footing load for test wall.**

## REINFORCEMENT RUPTURE CALCULATION

### Field-scale test wall:

**LATERAL STRESS RATIO:**

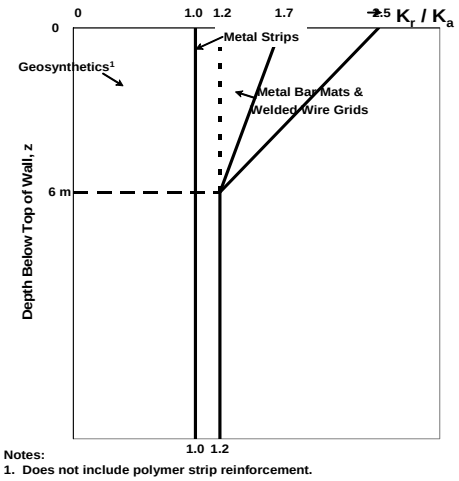


| Wall Parameters: | | |
|---|---|---|
| Wall height (m): | 5.5 | |
| Embedment depth (m): | 0 | |
| Soil unit weight (kN/m3): | 15.6 | |
| Wall batter (degrees): | 2.39 | (measured from vertical) |
| Inclination of facing (degrees): | 92.39 | (measured from horizontal in front of wall) |
| Friction angle (degrees): | 40 | |

Input Fields
Calculated Fields

| Reinforcement Input Parameters: | |
|---|---|
| Spacing ($s_v$)[1] (m): | 0.46 |
| Coverage Ratio ($R_c$): | 1 |
| Reinforcement type: | Geosynthetic |

***Calculation identical to Elias et al. (2)***

| Loading Input Parameters: | |
|---|---|
| Conc. vert. load, Fv (kN): | 0 |
| Conc. horiz. load, Fh (kN): | 0 |
| Uniform surcharge, q (kPa): | 0 |

| Earth Pressure Calculations: | |
|---|---|
| $K_a$ = | 0.217 |

| Layer (Bottom-upward): | z (m) | $K_r/K_a$[2] | $K_r$ | $\Delta\sigma_v$[3] (kPa) | $\sigma_v$ at reinforcement level (kPa) | $\Delta\sigma_h$[4] (kPa) | $\sigma_h$ at reinforcement level (kPa) | $T_i$ at reinforcement level (kN/m) |
|---|---|---|---|---|---|---|---|---|
| 1 | 5.5 | 1.00 | 0.217 | 79.5 | 165.3 | 0.0 | 35.9 | 16.5 |
| 2 | 5.04 | 1.00 | 0.217 | 80.8 | 159.5 | 0.0 | 34.7 | 16.0 |
| 3 | 4.58 | 1.00 | 0.217 | 82.7 | 154.1 | 0.0 | 33.5 | 15.4 |
| 4 | 4.12 | 1.00 | 0.217 | 85.6 | 149.9 | 0.0 | 32.6 | 15.0 |
| 5 | 3.66 | 1.00 | 0.217 | 88.6 | 145.7 | 0.0 | 31.7 | 14.6 |
| 6 | 3.2 | 1.00 | 0.217 | 92.4 | 142.3 | 0.0 | 30.9 | 14.2 |
| 7 | 2.74 | 1.00 | 0.217 | 97.1 | 139.8 | 0.0 | 30.4 | 14.0 |
| 8 | 2.28 | 1.00 | 0.217 | 103.4 | 139.0 | 0.0 | 30.2 | 13.9 |
| 9 | 1.82 | 1.00 | 0.217 | 110.8 | 139.2 | 0.0 | 30.3 | 13.9 |
| 10 | 1.36 | 1.00 | 0.217 | 120.1 | 141.3 | 0.0 | 30.7 | 14.1 |
| 11 | 0.9 | 1.00 | 0.217 | 140.0 | 154.0 | 0.0 | 33.5 | 15.4 |
| 12 | 0.44 | 1.00 | 0.217 | 210.2 | 217.1 | 0.0 | 47.2 | 21.7 |

**Notes:**
1. Vertical reinforcement spacing to be consistent with selection of wall facing.
2. Ratio to be input based on type of reinforcement selected and use of figure above.
3. Calculate the increment of vertical stress due to concentrated loads at the surface using the 2:1 method at each reinforcement layer.
4. Calculate the increment of horizontal stress (if any) due to concentrated loads at the surface.
5. Allowable tensile strength of reinforcement obtained from manufacturer specifications.

**Figure 79. Calculation. Reinforcement rupture calculation for test wall.**

***Step 4 – Calculate the pullout force.***

Calculate the pullout force, $T_{max}$, for MSE reinforcements in the resistant zone, as follows:

- The interior angle of the failure wedge: $\beta = 90 - \psi = 25^{o}$.
- Concentrated vertical load: $F_V = 890$ kN.
- No concentrated horizontal loads: $F_H = 0$ kN.
- Maximum surcharge loading: $q = 0$ kPa.
- For purposes of the calculation, assume the maximum MSE reinforcement length of 2.14 m.
- Calculate the pullout force per unit width of wall, $T_{max}$, using equation 14 in chapter 5.

The pullout force calculation is presented in figure 80. The pullout force was calculated as approximately 465 kN/m.

***Step 5 – Check the pullout resistance of MSE reinforcements in the resistant zone.***

Calculate the pullout resistance of the MSE reinforcements, and compare it to the required pullout capacity, $T_{max}$, calculated in step 4:

- Based on the reinforcement spacing, calculate the length of embedment of each reinforcement layer within the resistant zone per equation 18 in chapter 5. The embedment lengths are presented in figure 81.
- At each reinforcement layer within the resistant zone, calculate the pullout resistance, $F_{PO}$, according to equation 19 in chapter 5.
    - Because this calculation is conducted to calculate the factor of safety of the wall, use a factor of safety against pullout ($FS_p$) of one.
    - Assume $F^* = 0.8 \tan \phi'$ for geogrid reinforcement in granular soil ($F^* = 0.67$).
    - Reinforcement effective unit perimeter, $C = 2$.
    - Scale effect correction factor, $\alpha$, to account for a nonlinear stress reduction over the embedded length of highly extensible reinforcements. Use 0.8 for geogrids.
    - Coverage ratio, $R_c = 1$.
    - The vertical stress, $\sigma_v$, is equivalent to $\gamma H$.

**REQUIRED PULLOUT CAPACITY OF REINFORCEMENTS IN RESISTANT ZONE**

**Equations:**

$$T_{max} = \frac{L\left(\gamma\left(H - \frac{L}{2\tan\beta}\right) + q\right) + F_V}{\tan\left(\phi' + \beta\right)} + F_H$$

**Field-scale test wall:**

**FAILURE SURFACE APPROXIMATION:**

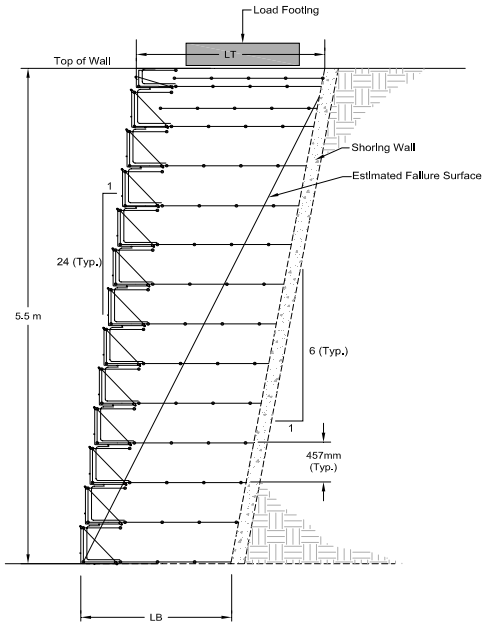


**FREE-BODY DIAGRAM:**

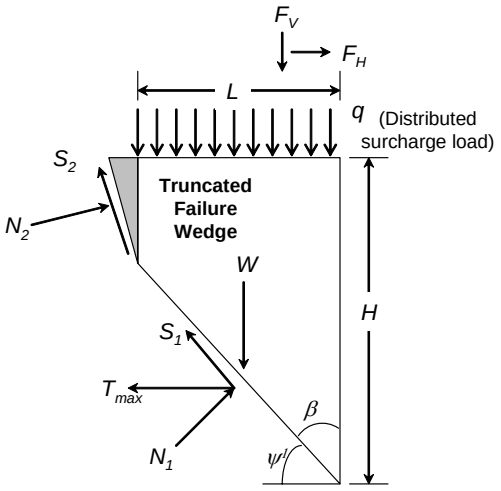


| ASSUMPTIONS: | |
|---|---|
| Wall height, H (m): | 5.5 |
| Wall length at top, $L_T$ (m): | 2.1 |
| Wall length at base, $L_B$ (m): | 1.4 |
| Shoring wall batter, 1H:?V: | 6 |
| Length of truncated wedge, L (m): | 2.1 |
| Soil unit weight (kN/m$^3$): | 15.6 |
| Friction angle (degrees): | 40 |

| LOADING: | |
|---|---|
| Conc. vert. load, $F_v$ (kN/m): | 890 |
| Conc. horiz. load, $F_H$ (kN/m): | 0 |
| Surcharge, q (kPa): | 0 |

| CALCULATIONS: | |
|---|---|
| β (degrees) = | 25.0 |
| **$T_{max}$(kN/m):** | 464.9 |

Input Fields
Calculated Fields

***Calculation unique to SMSE walls.***

**Figure 80. Calculation. Calculation of required pullout capacity for test wall.**

## CALCULATED PULLOUT RESISTANCE

### Field-scale test wall:

**FAILURE SURFACE APPROXIMATION:**

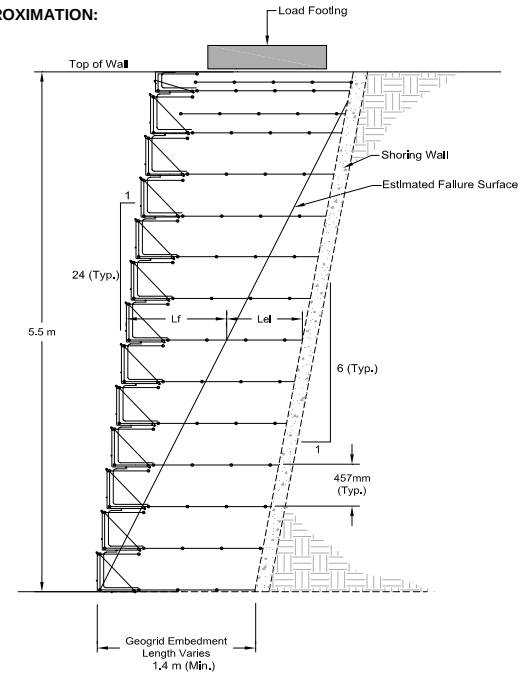


| Wall Parameters: | |
|---|---|
| Wall height (m): | 5.5 |
| Embedment depth (m): | 0 |
| Min. reinf. length, L (m): | 1.4 |
| Shoring wall batter (1H:?V): | 6 |
| MSE wall batter (1H:?V) | 24 |

Input Fields
Calculated Fields

| Soil Parameters: | |
|---|---|
| Soil unit weight (kN/m$^3$): | 15.6 |
| Friction angle (degrees): | 40 |
| $\psi$ (degrees): | 65 |

***Calculation unique to SMSE walls.***

| Reinforcement Input Parameters: | | |
|---|---|---|
| Calculation type (FS/Design): | FS | |
| Allowable strength (kN/m): | 52 | Tensar UX1500MSE |
| Ultimate strength (kN/m): | 114 | Tensar UX1500MSE |
| Spacing (s)[1] (m): | 0.46 | |
| Reinforcement type: | 1 | Type 1 = geogrid; Type 2 = geotextile |
| Scale effect factor, $\alpha$: | 0.8 | |
| Effective unit perimeter,C: | 2 | Taken as 2 for strips, grids, and sheets. |
| Pullout resistance factor,F*: | 0.67 | |
| Factor of safety, $FS_p$: | 1.0 | |
| Coverage ratio, $R_c$: | 1 | Taken as 1 for full coverage. Calculate for strips, etc. |

| Layer (Bottom-upward): | z (m) | L (m) | $L_f$ (m) | $L_{ei}$[1] (m) | Total $\sigma_v$ (kPa) | $F_{PO}$ (kN) |
|---|---|---|---|---|---|---|
| 1 | 5.5 | 1.40 | 0.00 | 1.40 | 85.8 | 114.0 |
| 2 | 5.04 | 1.46 | 0.20 | 1.26 | 78.6 | 106.8 |
| 3 | 4.58 | 1.52 | 0.39 | 1.13 | 71.4 | 86.7 |
| 4 | 4.12 | 1.57 | 0.59 | 0.98 | 64.3 | 67.9 |
| 5 | 3.66 | 1.63 | 0.78 | 0.85 | 57.1 | 52.0 |
| 6 | 3.2 | 1.69 | 0.98 | 0.71 | 49.9 | 38.2 |
| 7 | 2.74 | 1.75 | 1.17 | 0.58 | 42.7 | 26.5 |
| 8 | 2.28 | 1.80 | 1.37 | 0.43 | 35.6 | 16.5 |
| 9 | 1.82 | 1.86 | 1.56 | 0.30 | 28.4 | 9.1 |
| 10 | 1.36 | 1.92 | 1.76 | 0.16 | 21.2 | 3.7 |
| 11 | 0.9 | 1.98 | 1.95 | 0.03 | 14.0 | 0.4 |
| 12 | 0.44 | 2.03 | 2.03 | 0.00 | 6.9 | 0.0 |
| | | | | **Total pullout capacity (kN):** | | **522** |

**Notes:**
1. Length of reinforcement in resistant zone.

**Figure 81. Calculation. Calculation of pullout resistance for test wall.**

- Because this calculation is being conducted to evaluate the factor of safety of the MSE reinforcements against pullout, the ultimate tensile strength of the geogrid reinforcements (i.e., 114 kN/m) should be compared to the calculated pullout resistance instead of the allowable pullout resistance (i.e., 52 kN/m). Use of the ultimate pullout resistance removes factors of safety applied for creep, installation damage, and chemical/biological durability.

- The pullout resistances at each reinforcement level are summarized in figure 81. The total pullout capacity of the reinforcements of 522 kN/m is greater than the calculated pullout force, $T_{max}$, of 465 kN/m. The factor of safety against reinforcement pullout can be calculated using the following equation:

$$FS_p = \frac{\sum F_{PO}}{T} = \frac{522}{465} = 1.1 \qquad \textbf{Equation C.2}$$

  According to the design methodology presented in chapter 5, the field-scale test wall would not exhibit failure under the maximum test load, as observed from the load testing.

### C.9.2 Summary

Under the maximum test load, the design methodology presented in this report produces a factor of safety of 1.1 for pullout of the MSE reinforcements for the field-scale test. The factor of safety with regard to pullout was calculated using the ultimate strength of the MSE reinforcements instead of the allowable strength, as would have been considered in design. The factor of safety calculation for internal failure mechanisms of the test wall partially validates the design methodology presented in this report.

## C.10 CONCLUSIONS

Phase II of the centrifuge testing program predicted that failure of the field-scale test wall would not occur under a footing pressure of 239 kPa, which was the maximum achievable test load for the centrifuge model. The field-scale test wall was loaded to a maximum footing pressure of 356 kPa over a contact area of approximately 35 percent (i.e., 125 kPa) which is approximately equivalent to 10 times the normal traffic surcharge of 12 kPa. Even at this very high surcharge loading, the field-scale test wall did not exhibit failure.

Instrumentation data shows that the field-scale test wall did exhibit measurable strain and deformation as a function of the test load. The measured strains in the various geogrid layers were small, generally less than one percent which is well within the serviceability limits of the geogrid. Vertical and horizontal deformation of the MSE wall was also relatively small, with maximum settlements on the order of 16 mm and maximum horizontal deformations from 9 to 13 mm.

With the exception of data obtained from the vertical pressure cells where the uppermost load cell installed in the connected MSE section exhibited significantly higher lateral earth pressures, the connected and unconnected wall sections generally exhibited similar behavior.

The hypotheses established prior to load testing of the field-scale test wall were confirmed, as follows:

- Construction of an MSE wall in front of a rigid backslope (i.e., shoring system or stable rock face) results in reduced external lateral loading on the MSE wall compared to a conventional MSE wall. The lateral loading appears to be larger for a connected wall system.

Fully-connected wall systems appear to provide limited benefit for an SMSE system over an unconnected wall system, where the connected system appeared only to reduce the potential for tension crack development and nominally decrease lateral deformation.